Global Journal of Pure and Applied Mathematics.
ISSN 0973-1768 Volume 22, Number 2 (2026), pp. 279-298

https://dx.doi.org/10.37622/GJPAM/22.2.2026.279-298

Linear instability of convection-reaction flow in a non-isothermal vertical channel filled with porous medium

Aakash Kumar[1] **and Abhishek K. Sharma**[2]

[1]*Department of Mathematics, Patna University, Patna-800005, Bihar, India*
[2]*Department of Mathematics, B. N. College, Patna University, Patna-800004, Bihar, India*

Abstract

The instability of a parallel convection-reaction flow caused by an external pressure gradient and buoyancy force in a vertical channel that is differentially heated and filled with a fluid-saturated high permeability porous media has been investigated using linear stability analysis. The volume averaged Navier-Stokes (VANS) equation is used as the governing equation. The Chebyshev spectral collocation method that uses Chebyshev polynomials as the basis functions is used to numerically solve the generalized eigenvalue problem pertaining to the linearized disturbance equations. The effect of chemical reaction parameter in terms of Damkohler number (k) and buoyancy ratio (N) on the instability of the basic flow is investigated. It is found that the basic flow exhibits a highly stable nature for $N = -1$, irrespective of the value of media permeability. The shear production of disturbance kinetic energy due to Reynolds stress is the most important factor behind this instability of the basic flow. The chemical reaction parameter in terms of Damkohler number (k) tends to stabilize the flow in high permeability porous medium whereas it has opposite effect in the case of relatively low permeability porous medium.

Keywords : Linear stability, Mixed convection, Parallel flow, Porous medium, Spectral collocation method.

Corresponding author, E-mail address: aakashpsc@gmail.com

1. INTRODUCTION

Double-diffusive is the term used to describe the buoyancy-driven flows caused by simultaneous concentration and temperature gradients.[1] Kaloni et al.[2] have theoretically explored the problem of continuous nonlinear double-diffusive convection in a porous medium employing the Brinkman-Forchheimer model. Applications of double-diffusive convection are present in scientific fields such as chemical processes, astrophysics, biology, geophysics, oceanography, geology (see for instance[1,2]) As demonstrated by Chamkha,[1] this possesses a wide variety of technological and engineering uses, including geothermal reservoirs, chemical catalytic reactors, exchangers for heat regeneration made of porous materials, diffusion of radioactive waste and other contaminants underground, petroleum extraction and pollution prevention.The impact of chemical reactions on the start of convection in porous media were initially studied by Steinberg and Brand,[3] but because their investigation was limited to extremely rapid chemical reactions, they overlooked solutal diffusion. Investigation of combined convective heat and mass transport in vertical systems is extremely important and frequently encountered in a variety of natural environments and practical applications, according to a recent study by Khandelwal et al.[4]

The simultaneous presence of mass and heat have many natural processes and important engineering or industrial applications such as chemical vapour deposition procedures, cooling towers, chemical distilleries, metal solidification processes, cooling of microelectronic equipment, channel type solar energy collectors and thermal protection systems. Heat transmission and fluid flow in porous media are regarded as two-phase problems. The saturated fluid in the void part of porous medium is one phase and the solid portion of porous matrix is another phase.[5] A substantial quantity of articles[6–18] are discussed in the literature using double-diffusive mixed convection flow to explore the findings in the liquid films on the walls for air-water and air-ethanol system to comprehend the properties of mass and heat movement in a vertical channel. With an analytical approach, El-Din[19] investigates a completely developed thermo-solutal mixed convection flow with constant concentration and temperature on the channel walls. Chamkha[20] demonstrated how the flow of a uniformly stretched vertical permeable surface is influenced by heat generation and absorption. Chen[21] studied the combined effects of mass and heat transmission in free convection in nature that is magnetohydrodynamic (MHD) on a vertical plate. In a different analytical technique, Boulama and Galanis[22] employed two different thermal boundary conditions: uniform fluxes of heat and uniform temperature of the walls with a uniform concentration on each of the walls.[23,24] Boulama et al.[22] investigated the same problem by taking into account the entropy generation and found that it depends on the solutal and thermal boundary conditions on the channel wall. The onset of thermosolutal (double-diffusive) convection of a binary fluid in a horizontal porous layer, subject to chemical equilibrium on the bounding surfaces and fixed temperatures, was examined by Pritchard et al.[25] Thermophoretic transport of small particles in a vertical channel for a fully developed mixed convection flow was examined by Grosan et al.[26] Thermophoretic effect was significant on flow dynamics as found by

them. Aldoss and Al-Nimir[27] studied the effect of local acceleration over a vertical plate on MHD transient convectional free flow. Ahmed et al.[28] investigated how transient free convective MHD flow along an infinite vertical porous plate is affected by viscous dissipation and chemical responsiveness. Malashetty[29] investigated the commencement of double diffusive reaction-convection in a horizontal anisotropic porous layer saturated with binary mixture using linear and non-linear stability analysis. The layer is heated and salted from below, and chemical equilibrium is maintained at the boundaries. Mohammed et al.[30] examined the mixed convection heat and mass transfer for an air-water system in a vertical channel with uniform but distinct heat fluxes. They also found that increase in vapor concentration and ambient temperature of humid air enhances the condensation rate. Bennon and Incropera conducted an experimental and computational research for the mixed convection solidification of a binary aqueous ammonium chloride solution in a vertical channel. The solidification in binary substances is associated with the complex phenomena is supported by the experimental study. The majority of the results in laminar mixed convection of heat and mass transmission in a vertical channel are due to liquid film evaporation and condensation. Few researchers have studied chemical reactions involving mixed convective heat and mass transfer in vertical channels.[31]

To the best of our knowledge the instability of a mixed convection-reaction flow in a vertical channel filled with porous medium saturated with a binary fluid is not investigated yet. So, an attempt has been made in this direction.

Nomenclature	
t	time
$\mathbf{v}$	Darcy velocity vector
(x, y, z)	space coordinates
g	gravitational acceleration
K	permeability
k_c	solutal diffusivity
k_T	thermal diffusivity
$\hat{k}$	effective reaction rate
P	pressure
C	concentration
k	Damköhler number = $\frac{\hat{k}L^2}{\epsilon k_T}$
N	ratio of buoyancy forces = $\frac{\beta_C(C_1-C_2)}{\beta_T(T_1-T_2)}$
Gr	Grashof number = $\frac{g\beta_T(T_2-T_1)L^3}{\nu^2}$
Gr'	=$\frac{Gr}{Re^2}$
Da	Darcy number = $\frac{K}{L^2}$
Pr	Prandtl number = $\frac{\nu}{k_T}$
Re	Reynolds number = $\frac{\vec{V_0}L}{\nu}$
Sc	Schmidt number = $\frac{\nu}{k_c}$

Greek symbols	
β_T	thermal expansion coefficient
β_C	solutal expansion coefficient
ε	porosity
$\tilde{\mu}$	effective viscosity
μ_f	fluid viscosity
ν	kinematic viscosity
ρ	fluid density
ρ_f	fluid density at reference state
θ	temperature

2. MATHEMATICAL FORMULATION

2.1. Problem formulation and governing equations

The present study is carried out to identify the instability mechanism behind the double diffusive mixed convection-reaction flow in an infinite long vertical channel filled with a porous medium that is saturated with a reactive binary fluid as shown in Figure 1. Further, chemical equilibrium holds at the boundaries[25] such that the thermal contribution of the reaction is ignored without affecting the permeability of the porous medium.

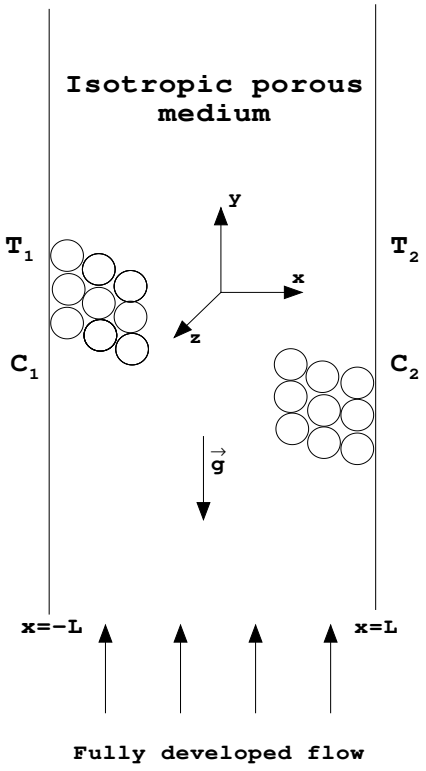

Figure 1: Schematic of the physical problem

The fluid is modelled as a Boussinesq fluid such that $\rho = \rho_f[1 - \beta_T(T - T_0) - \beta_C(C - S_0)]$, where $T_0 = (T_1 + T_2)/2$ is the mean temperature and $S_0 = (C_1 + C_2)/2$ is the mean concentration. The momentum balance equation for the aforementioned flow is determined by applying Whitaker's[32] volume averaged Navier-Stokes (VANS) equation. The dimensional governing equations are expressed as

$$\nabla.\mathbf{v} = 0, \tag{2.1}$$

$$\rho_f\left[\frac{1}{\epsilon}\frac{\partial \mathbf{v}}{\partial t}+\frac{1}{\epsilon^2}(\mathbf{v}.\nabla)\mathbf{v}\right]=-\nabla P+\rho\vec{g}+\tilde{\mu}\nabla^2\mathbf{v}-\frac{\mu_f}{K}\mathbf{v}, \tag{2.2}$$

$$\sigma\frac{\partial T}{\partial t}+(\mathbf{v}.\nabla)T=k_T\nabla^2 T, \tag{2.3}$$

$$\epsilon\frac{\partial C}{\partial t}+(\mathbf{v}.\nabla)C=\epsilon k_c\nabla^2 C+\hat{k}(C_{eq}(T)-C). \tag{2.4}$$

The corresponding boundary conditions over the walls of the channel are given as:

$$\mathbf{v}=0, T=\pm 1/2, C=\pm 1/2 \;\; at \;\; x=\pm 1. \tag{2.5}$$

where, $C_{eq}(T)=S_0+\frac{C_2-C_1}{T_2-T_1}(T-T_0)$ is the equilibrium solute concentration. The non-dimensional quantities: $(x^*,y^*,z^*)=(1/L)(x,y,z)$, $t^*=t\frac{\overline{V_0}}{L}$, $\mathbf{v}^*=\frac{\mathbf{v}}{\overline{V_0}}$, $\theta=\frac{T-T_0}{T_2-T_1}$, $C^*=\frac{C-S_0}{C_2-C_1}$, $P^*=\frac{P}{\rho_f\overline{V_0^2}}$ after the asterisk is dropped, lead to the non-dimensional governing equations as follows:

$$\nabla.\mathbf{v}=0, \tag{2.6}$$

$$\frac{1}{\epsilon}\frac{\partial \mathbf{v}}{\partial t}+\frac{1}{\epsilon^2}(\mathbf{v}.\nabla)\mathbf{v}=-\nabla P+\frac{\Lambda}{Re}(\nabla^2\mathbf{v})-\frac{1}{DaRe}\mathbf{v}+Gr'(\theta+NC)\hat{e_y}, \tag{2.7}$$

$$\sigma\frac{\partial \theta}{\partial t}+(\mathbf{v}.\nabla)\theta=\frac{1}{PrRe}(\nabla^2\theta) \tag{2.8}$$

$$\frac{\partial C}{\partial t}+\frac{1}{\epsilon}(\mathbf{v}.\nabla)C=\frac{1}{ScRe}\nabla^2 C+\frac{k}{PrRe}(\theta-C) \tag{2.9}$$

with boundary conditions given as:

$$\mathbf{v}=0, \theta=\pm 1/2, C=\pm 1/2 \;\; at \;\; x=\pm 1, \tag{2.10}$$

The literature[33] reports varying values for $\tilde{\mu}$ leading to a Λ other than unity. In the study, however, Λ= 1 has been used as there isn't a definite observed value. Owing to the absence of a precise determined value for $(\rho c_m)_m$ where there is considerable porosity in this study, σ = 1 is considered.

2.2. Parallel flow: Basic State

The governing equations (2.6) to (2.9) along with the boundary conditions (2.10) are converted into a set of ordinary differential equations referred as basic flow assuming that it is fully developed, steady-state, and unidirectional in the vertical channel. The basic flow equations are obtained as

$$\frac{d^2V_0}{dx^2}-\frac{V_0}{Da}+Gr'(\theta_0+NC_0)=Re\frac{dP_0}{dy} \tag{2.11}$$

$$\frac{d^2\theta_0}{dx^2}=0 \tag{2.12}$$

$$\frac{1}{Sc}\frac{d^2C_0}{dx^2} + \frac{k}{Pr}(\theta_0 - C_0) = 0 \tag{2.13}$$

with boundary conditions for these basic state equations as:

$$V_0 = 0, \theta_0 = \pm 1/2, C_0 = \pm 1/2 \ \ at \ \ x = \pm 1, \tag{2.14}$$

Here, V_0, θ_0, C_0 and P_0 are the basic velocity, basic temperature, basic concentration and basic pressure, respectively.

To solve the equations (2.11)–(2.14), the axial pressure gradient is determined using the global mass conservation, $\int_{-1}^{1} V_0 dx = 2$. A comparative graph of basic flow velocity is presented in figure 2 for four different values of $\{10^{-1}, 10^{-2}, 10^{-3}, 10^{-4}\}$ of Darcy number (Da). In each case the velocity profiles are drawn for three different values $-2, 0, 1$ of the buoyancy ration (N). A common phenomenon that can be observed in each case is that for relatively smaller values of Gr', the velocity profile is free from back flow and point of inflection, showing that the flow is primarily due to external pressure gradient as the temperature difference between the walls is negligible. On the other hand, for relatively higher values of Gr', the velocity profiles possess back flow and point of inflection, irrespective of the value of the buoyancy ratio N. It can be seen that for Gr' greater than or equal to 250 the points of inflection start appearing in the basic velocity profile when N = -2 or 0. The same happens for $Gr' > 124$ when $N = 1$ representing the potential for instability in the flow. The thickness of the boundary layer tends to decrease on increasing the value of Gr'. The maximum value of the basic velocity increases on increasing the value of Gr'. The same observation is made for other set of parametric values also. For example, on increasing the value of Gr' when $Da = 10^{-1}$, the curve changes its shape from parabolic form and gives first and second inflection points at $Gr' = 43, 43, 22$ and $Gr' = 60, 80, 40$ for $N = -2, 0,$ and 1 respectively. The appearance of point of inflection and back flow in the velocity profile is a potential for instability.[34] Thus, the next section will carry out temporal linear stability analysis of the basic flow.

2.3. Temporal linear stability

To investigate the linear stability of the aforementioned basic flow, an infinitesimal disturbance dependent on time is applied. Thus, the basic state and a infinitesimal perturbation are separated from the field variables, as

$$(\mathbf{v}, \theta, C, P) = (V_0(x)\hat{e}_y, \theta_0(x), C_0(x), P_0(y)) + (\mathbf{v}', \theta', c', p') \tag{2.15}$$

The normal mode from[34] is formed by separating these infinitesimal disturbances of the corresponding field variables as follows:

$$(\mathbf{v}', \theta', c', p') = (\hat{\mathbf{v}}(x), \hat{\theta}(x), \hat{C}(x), \hat{p}(x))e^{i(\alpha y + \beta z - \alpha c t)} \tag{2.16}$$

where, α and β are the wavenumbers in streamwise and spanwise directions respectively, and $c = c_r + ic_i$ is a complex wave speed. The disturbances are classified

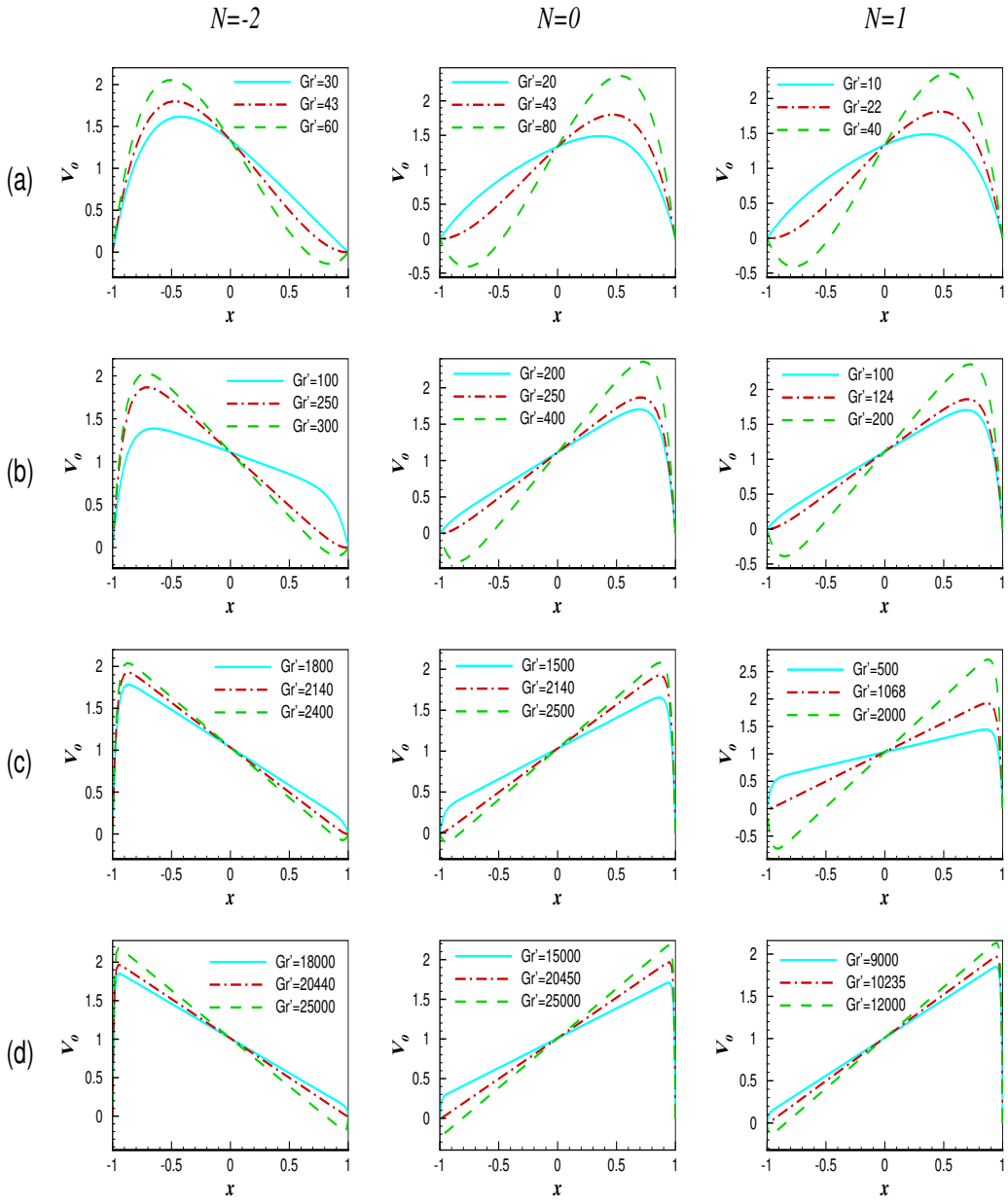

Figure 2: Basic velocity profiles for (a) $Da = 10^{-1}$ (b) $Da = 10^{-2}$ (c) $Da = 10^{-3}$ (d) $Da = 10^{-4}$ when $Pr = 0.7, Sc = 1, k = 1$.

as stable, neutrally stable, or unstable depending on whether $c_i < 0$, $c_i = 0$, or $c_i > 0$, respectively. On substituting the equations (2.15) and (2.16) into the governing equations (2.6)–(2.9), subtracting the equations (2.11) to (2.13), and after eliminating the pressure, the linear equations for the infinitesimal disturbances are given as,

$$\frac{d\hat{u}}{dx} + i\alpha\hat{v} + i\beta\hat{w} = 0 \tag{2.17}$$

$$\frac{d\theta_0}{dx}\hat{u} + i\alpha(V_0 - c)\hat{\theta} - \frac{1}{PrRe}\left(\frac{d^2\hat{\theta}}{dx^2} - (\alpha^2+\beta^2)\hat{\theta}\right) = 0 \tag{2.18}$$

$$i\alpha Re\frac{1}{\epsilon}\left(\frac{1}{\epsilon}V_0 - c\right)\hat{\eta} + \beta Re\frac{1}{\epsilon^2}\frac{dV_0}{dx}\hat{u} - \frac{d^2\hat{\eta}}{dx^2} + (\alpha^2+\beta^2)\hat{\eta} + \frac{1}{Da}\hat{\eta} - \beta Gr'(\hat{\theta} + N\hat{C}) = 0 \tag{2.19}$$

$$\frac{d^4\hat{u}}{dx^4} - 2(\alpha^2+\beta^2)\frac{d^2\hat{u}}{dx^2} + i\alpha Re\frac{1}{\epsilon^2}\frac{d^2V_0}{dx^2}\hat{u} + (\alpha^2+\beta^2)^2\hat{u} - i\alpha Gr'\left(\frac{d\hat{\theta}}{dx} + N\frac{d\hat{C}}{dx}\right) + \left(i\alpha cRe\frac{1}{\epsilon} - \frac{1}{Da} - i\alpha Re\frac{1}{\epsilon^2}V_0\right)\left[\frac{d^2\hat{u}}{dx^2} - (\alpha^2+\beta^2)\hat{u}\right] = 0 \tag{2.20}$$

$$\frac{1}{\epsilon}\frac{dC_0}{dx}\hat{u} + i\alpha(V_0 - c)\hat{C} - \frac{1}{ScRe}\left(\frac{d^2\hat{C}}{dx^2} - (\alpha^2+\beta^2)\hat{C}\right) + \frac{k}{RePr}(\hat{\theta} - \hat{C}) = 0 \tag{2.21}$$

where, $\hat{\eta} = \beta\hat{v} - \alpha\hat{w}$. The boundary conditions for the disturbances are given as

$$\hat{u} = \frac{d\hat{u}}{dx} = \hat{\theta} = \hat{\eta} = \hat{C} = 0 \; at \; x = \pm 1. \tag{2.22}$$

As a generalized eigenvalue problem, the above mentioned linear disturbance equations and homogeneous boundary conditions are expressed as follows:

$$AX = cBX \tag{2.23}$$

where A and B are the square complex matrices of order $4N+4$, where N is the order of the base polynomial in the collocation method, complex wavespeed c is the eigenvalue, and X is the representation of the eigenfunctions involved. The intricate QZ technique integrated within MATLAB through eig command is used to find the eigenvalues of the system mentioned above.To solve the set of coupled ordinary differential equations arising in this study, we have employed the Chebyshev spectral collocation method, which uses Chebyshev polynomials as the basis functions, to discretize the system of differential equations and their boundary conditions in the interval $[-1, 1]$ along x-direction at Gauss-Lobatto points. The Gauss-Chebyshev quadrature formula is used to calculate the integrals throughout the entire calculations.

The convergence of the numerical scheme and grid independence is verified by varying the order N of the Chebyshev base polynomial and ensuring that the change in the least stable eigenvalue by Chebyshev collocation method becomes negligible $(O(10^{-6}))$, see table 1.

Table 1: Convergence of the least stable eigenvalue by Chebyshev collocation method at $Pr = 0.7$; $\epsilon = 0.9$; $Sc = 1$; $k = 1$; $Re = 1000$; $Da = 10^{-2}$; $N = 1$; $\beta = 0$; $\alpha = 0.1$.

N	Least stable eigenvalue
20	1.102327780442677 - 0.013370401454131i
30	1.102328980697384 - 0.013369639920627i
40	1.102329389983527 - 0.013366283047606i
50	1.102353913447135 - 0.013354339914972i
55	1.102353005334885 - 0.013366466953965i
60	1.102353062368277 - 0.013366458860618i

3. RESULTS AND DISCUSSION

In the present study, we have carried out a detailed study of the linear instability mechanism of a double diffusive mixed convection-reaction flow in a porous medium. The values of certain parameters are fixed. The porosity and heat capacity ratio are kept constant at 0.9 and 1, respectively. Here, four different values ($10^{-1}, 10^{-2}, 10^{-3}$ and 10^{-4}) of Da and three different values ($-2, 0$ and 1) of N are taken to carry out a wide range of study.

The linear instability boundaries as a function of Reynolds number (Re) are plotted in figure 3 depicting the critical values of Gr', for different values of Da considered in this study, when $N = 1, Pr = 0.7, Sc = 1$ and $k = 1$. A common phenomenon that can be observed in figure 3 is that there is a sharp fall in the critical values of Gr' up to a threshold value of $Re = 300$. Afterwards, the graph becomes almost horizontal after and only a small gradual change is seen in the graph as the value of Re is increased beyond the threshold value, except the case when $Da = 10^{-1}$ where again a sharp fall in the critical values of Gr' is observed after $Re = 10^4$. The stability of the basic flow decreases with an increase in the value of Re and as a result the critical value of Gr' also reduces. The relative critical value of Gr' increases by almost one order as we decrease the value of Da by one order as can be seen from the figures 3(a)-(d), suggesting that the effect of increasing media permeability is to destabilize the flow. The basic flow becomes unstable even at very low values of Gr' when $Da = 10^{-1}$. For instance the critical value of Gr' is 225 when $Re = 10$. This instability of the basic flow can be explained through the shear production of disturbance kinetic energy due to Reynolds stress as we shall see further in the result section.

A very interesting observation is made in figure 4 as the instability boundary is drawn in the (N, Gr') plane. As can be seen from the figure, a vertical peak in the critical Gr' is observed near $N = -1$ highlighting the highly stable nature of the basic flow when the buoyancy ratio is equal to -1 as compared to other near by values of buoyancy ratio N for all the four cases of considered values of Da. The two buoyant forces, one arising due to temperature gradient and the other due to concentration gradient, are equal in magnitude but opposite in direction when $N = -1$. In this case the basic velocity profile is independent of the value of Gr'. It is parabolic in shape free from any

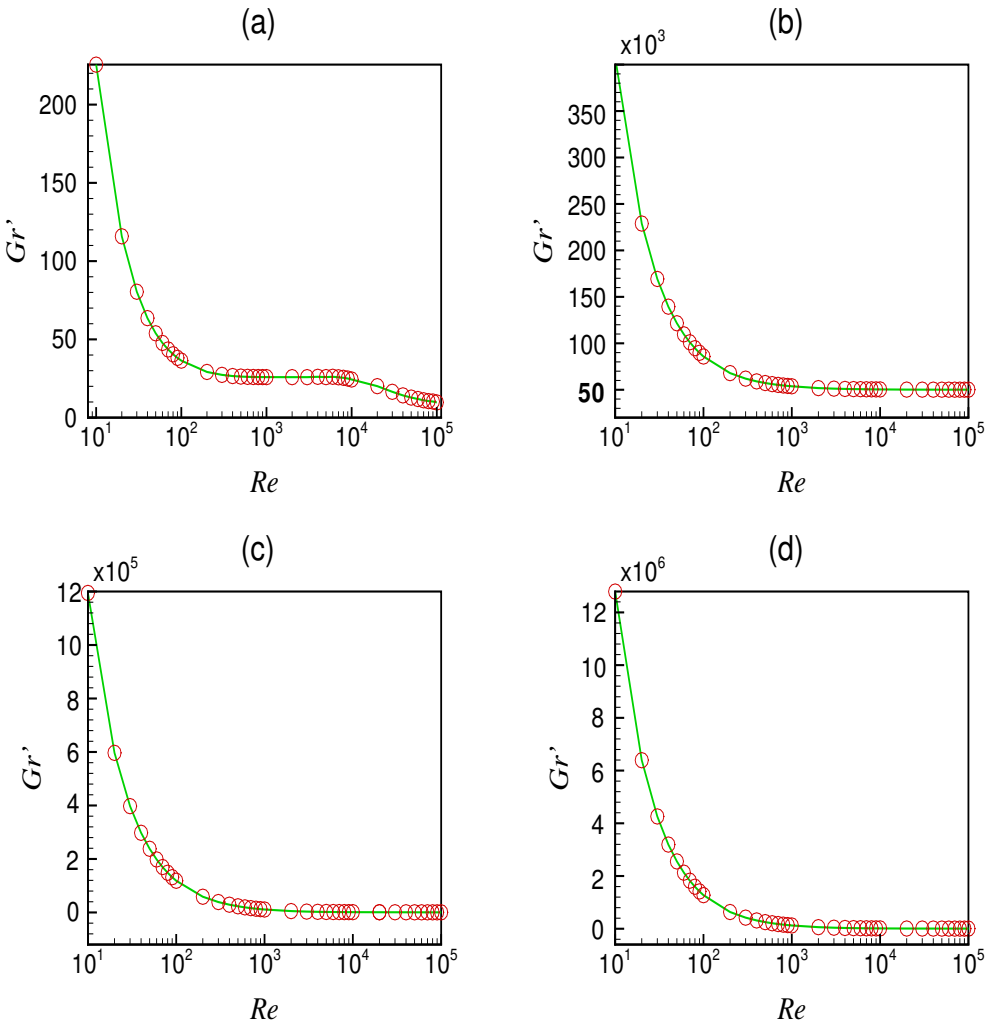

Figure 3: Linear instability boundaries in the (Re, Gr') plane for (a) $Da = 10^{-1}$ (b) $Da = 10^{-2}$ (c) $Da = 10^{-3}$ (d) $Da = 10^{-4}$ when $N = 1, Pr = 0.7, Sc = 1, k = 1$.

point of inflection or back flow. Thus the basic flow exhibits a highly stable nature when $N = -1$ irrespective of the value of media permeability. The instability boundary curve decreases sharply on both sides as we move away from $N = -1$ showing a decrease in the stability of the basic flow for the considered set of parameters.

The chemical reaction has a slightly subtle effect on the instability boundaries as shown in the figure 5. In case of $Da = 10^{-1}$, the linear instability boundaries are almost independent of the value of Damkohler number (k) up to $k = 15$, beyond which a sudden rise in the critical values of Gr' occurs before $k = 20$. When the media permeability is decreased by one order, i.e. $Da = 10^{-2}$, although the basic flow is relatively more stable but the dependency on the Damkohler number is not as straightforward as the case when $Da = 10^{-1}$. The critical value of Gr', increases on increasing the value of k except for a subdomain of k $(0 < k < 6)$. A slight

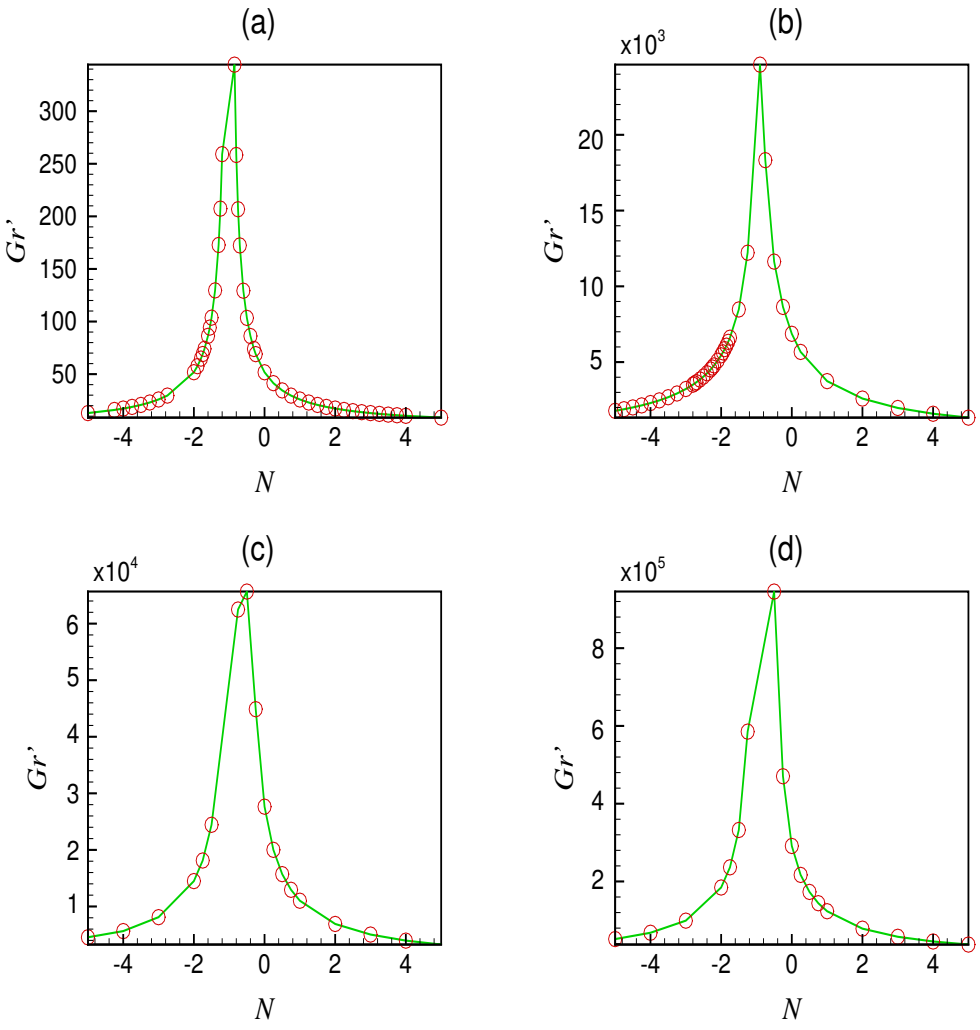

Figure 4: Linear instability boundaries in the (N, Gr') plane for (a) $Da = 10^{-1}$ (b) $Da = 10^{-2}$ (c) $Da = 10^{-3}$ (d) $Da = 10^{-4}$ when $Re = 1000, Pr = 0.7, Sc = 1, k = 1$.

growth in critical Gr' is seen from $k = 7$ up to 10. After $k = 16$ a sudden rise in the value of critical Gr' is observed. The instability boundary curves show that the chemical reaction parameter in general stabilises the basic flow when $Da = 10^{-1}$ and 10^{-2}. For relatively low media permeability, i.e. $Da = 10^{-3}$ and 10^{-4}, the instability boundaries show a decreasing trend with respect to the chemical reaction parameter showing a destabilizing effect of the Damkohler number. The figure 6 shows the linear instability boundaries showing that making a porous medium less permeable makes the flow much more stable against thermal changes. In the subplots, 6 (a) to 6 (d), Da decreases, meaning the porous matrix becomes less permeable and more tightly packed. For $Da = 10^{-1}$ (a) and $Da = 10^{-2}$ in (b), the critical Gr' is relatively low ($\sim$ 10 to 15). However, as permeability drops significantly in (c) and especially (d) where $Da = 10^{-4}$, the critical Gr' goes up to approximately 150. The curves show the

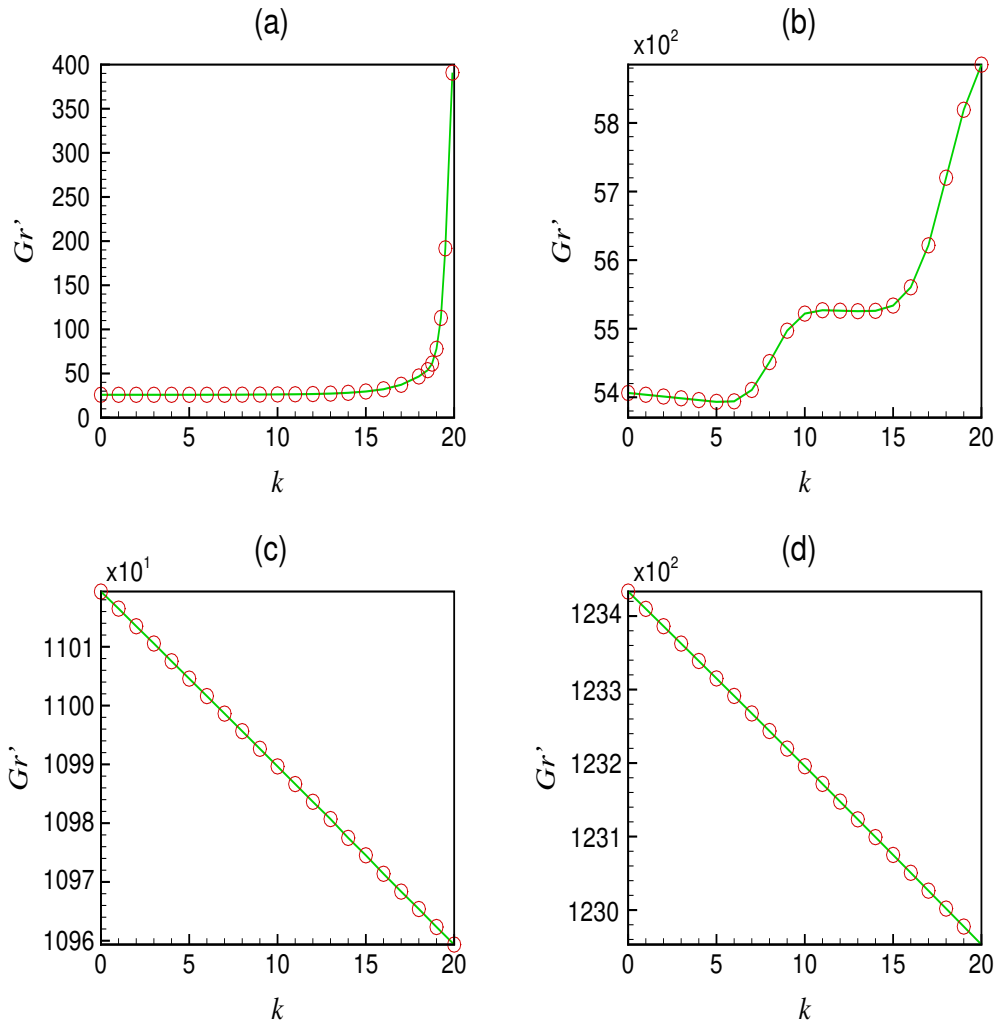

Figure 5: Linear instability boundaries in the (k, Gr') plane for (a) $Da = 10^{-1}$ (b) $Da = 10^{-2}$ (c) $Da = 10^{-3}$ (d) $Da = 10^{-4}$ when $N = 1, Re = 1000, Pr = 0.7, Sc = 1$.

neutral stability threshold, which is the point at which the growth rate of perturbations is exactly zero.

The production and dissipation of disturbance kinetic energy (KE) can be used to determine the driving processes of flow instability. The balance of KE is as follows:[35]

$$Re\frac{1}{\epsilon}\frac{\partial}{\partial t}\left\langle\frac{1}{2}(u'^2+v'^2+w'^2)\right\rangle =$$
$$-Re\frac{1}{\epsilon^2}\left\langle u'v'\frac{dV_0}{dx}\right\rangle + Gr' < v'\theta' > -\frac{1}{Da} < u'^2+v'^2+w'^2 > -\left\langle(\nabla u')^2+(\nabla v')^2+(\nabla w')^2\right\rangle$$
$$= E_s + E_b + E_D + E_d \tag{3.1}$$

The symbol <> represents integration over the volume [-1,1] x $[0, \frac{2\pi}{\alpha}]$ x $[0, \frac{2\pi}{\beta}]$ of

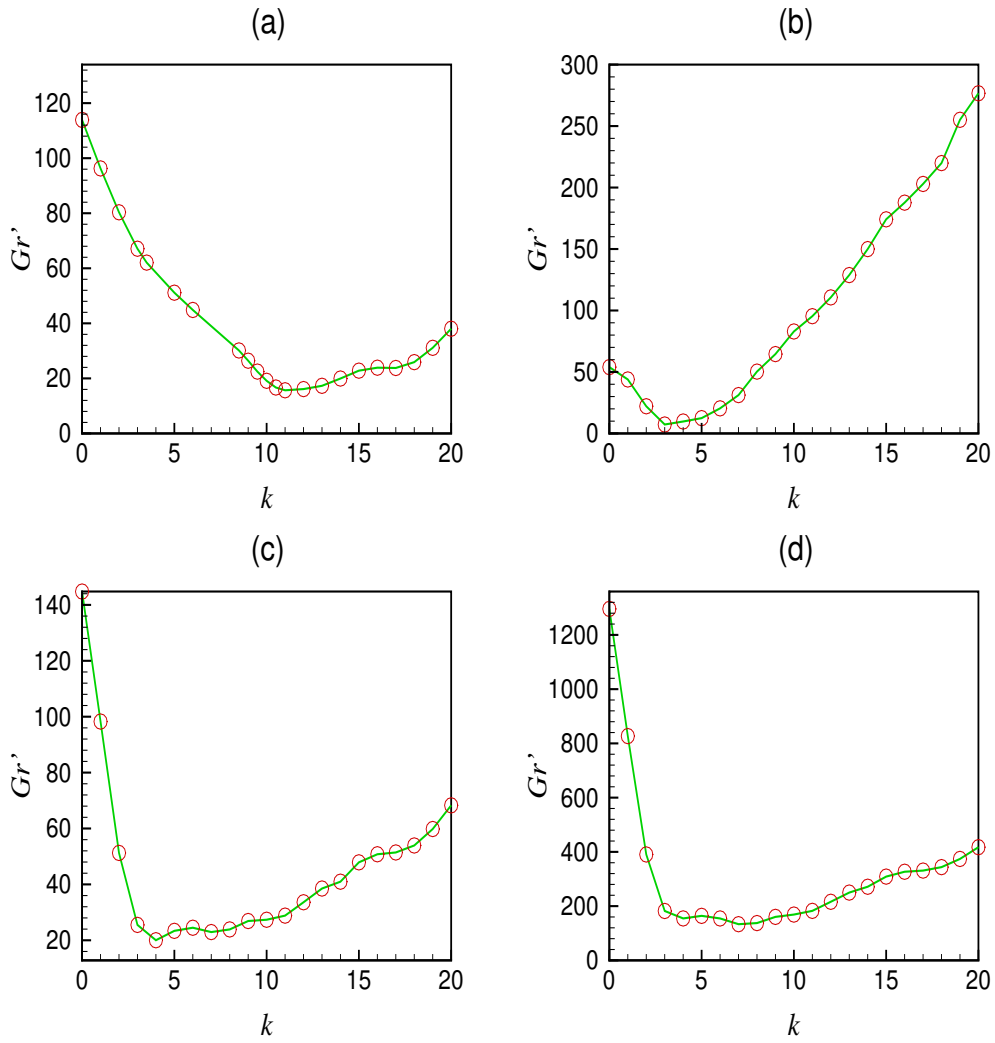

Figure 6: Linear instability boundaries in the (k, Gr') plane for (a) $Da = 10^{-1}$ (b) $Da = 10^{-2}$ (c) $Da = 10^{-3}$ (d) $Da = 10^{-4}$ when $N = -1, Re = 1000, Pr = 0.7, Sc = 1$.

the disturbance cell. On the curve of neutral stability, the disturbances do not grow or decrease, and the left-hand side of (3.1) is zero. Here, E_s represents shear production or destruction through Reynolds stress; E_b, reflects the production of disturbance KE through work done by the variable body force; (E_D) describes the dissipation of disturbance KE caused by surface drag; and (E_d) represents the dissipation of energy owing to viscous processes. As a result, equation (3.1) shows a balance between the creation of KE by the buoyant and shear mechanisms and its dissipation by surface drag and viscous action.

To shed more light into the instability mechanism of the basic flow, the disturbance KE balance at the critical point is studied which provides more insight into the instability mechanism of the basic flow. Figure 7 shows the disturbance KE balance in three

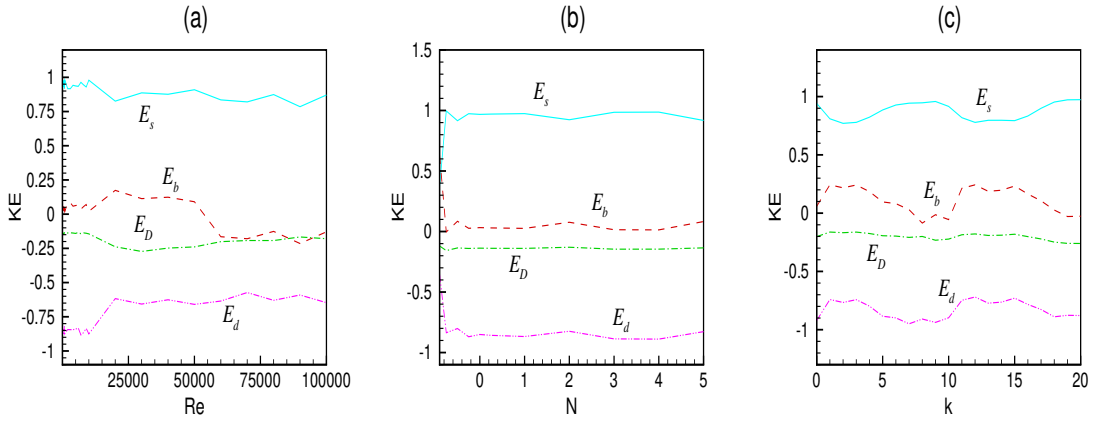

Figure 7: Disturbance KE balance as a function of (a) Re when $N = 1, k = 1$ (b) N when $Re = 1000, k = 1$ (c) k when $N = 1, Re = 1000$. In all the figures $Pr = 0.7, Sc = 1$ and $Da = 10^{-2}$.

different cases. First, as a function of Re, then as a function of N and lastly as a function of k. Here, the effect of production of disturbance energy due to buoyant term (E_b) and dissipation of disturbance energy due to surface drag (E_D) are negligible as compared to the shear production of disturbance energy (E_s) due to Reynolds stress and viscous dissipation of disturbance energy (E_d), respectively. The production of disturbance energy due to shear term (E_s) and the destruction of disturbance energy due to viscous dissipation (E_d) are positive and negative respectively, tending to balance each other. While E_s is responsible for destabilizing the fluid flow, E_d is tends to neutralize the destabilizing effect of E_s and helps in stabilizing the basic flow.

Further, figure 8 shows the disturbance stream function for different values of Da. As can be seen from the above figure that the disturbance contours propagate in the whole width of the channel in case of $Da = 10^{-1}$. But, as the permeability of the porous medium is reduced the disturbance stream function contours get more localised near the hot wall of the vertical channel having a bi-cellular pattern. These disturbances are damped out so that the magnitude of the disturbance stream function also decreases on increasing the permeability of the porous medium, when other parameters are kept fixed, validating the result obtained in figure 3 which showed an increase in the critical value of Gr' on reducing the value of Da. It would be interesting to understand how these localised disturbances interact with the boundary layer eventually leading to turbulence. Figure 9 shows the disturbance temperature function for a wide range of Darcy numbers. The disturbances are highly concentrated near the hot wall of the channel at $x = 0.6$. The maximum magnitude of the disturbances decrease on reducing the value of Darcy number which results in an increase in the critical value of Gr'.

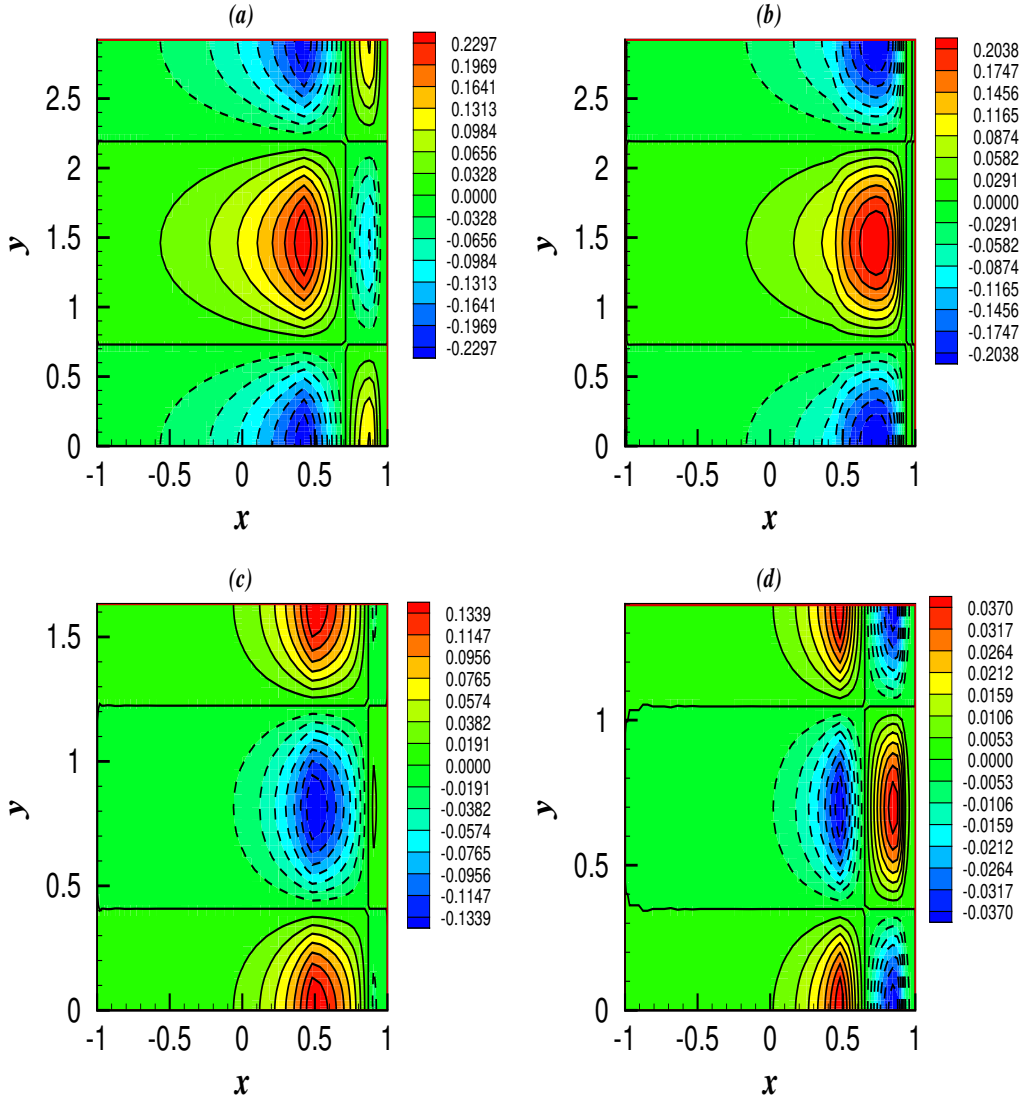

Figure 8: Disturbance stream function for (a) $Da = 10^{-1}$, (b) $Da = 10^{-2}$, (c) $Da = 10^{-3}$, (d) $Da = 10^{-4}$ when $Re = 1000, Pr = 0.7, Sc = 1, k = 1$.

4. CONCLUSION

We investigated the linear instability mechanism of a parallel mixed convection-reaction flow in a non-isothermal vertical channel filled with an incompressible binary fluid saturated porous medium under local thermal equilibrium state. The non-Darcy volume averaged Navier-Stokes equation is utilized as the governing equation. We have made an attempt to study the linear instability boundaries in the (Re, Gr')-plane, (N, Gr')-plane, (k, Gr')-plane. Also, the disturbance kinetic energy balance at the critical point is studied to identify the major disturbance forces responsible for stabilizing/destabilizing the basic flow. It has been found that for relatively higher

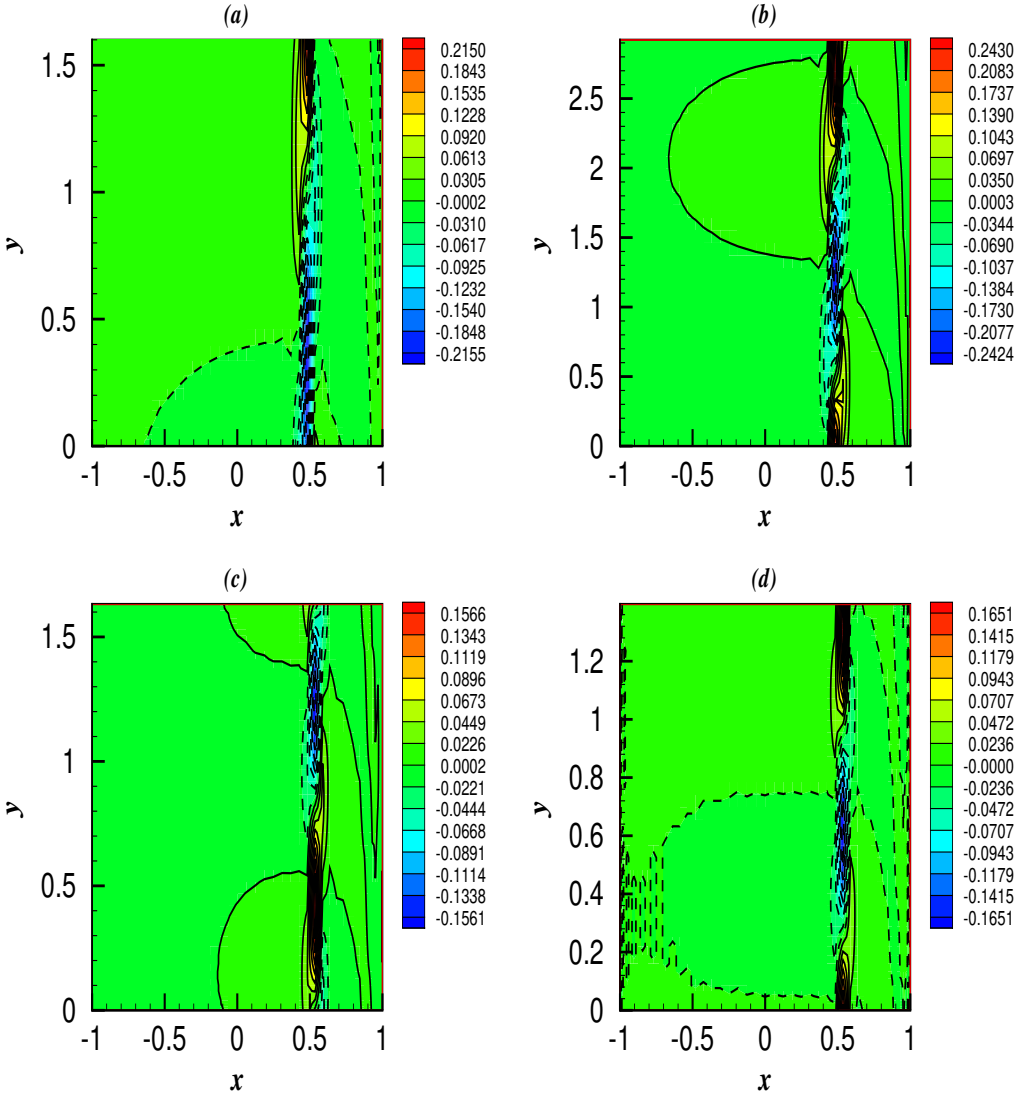

Figure 9: Disturbance temperature function for (a) $Da = 10^{-1}$, (b) $Da = 10^{-2}$, (c) $Da = 10^{-3}$, (d) $Da = 10^{-4}$ when $Re = 1000, Pr = 0.7, Sc = 1, k = 1$.

values of Gr', the velocity profiles possess back flow and point of inflection, irrespective of the value of the buoyancy ratio N, showing potential for instability. Further, the basic flow becomes unstable even at very low values of Gr' for relatively higher values of Darcy number. For instance the critical value of Gr' is 225 when $Da = 10^{-1}$ and $Re = 10$. The shear production of disturbance kinetic energy due to Reynolds stresses is the most important factor behind this instability of the basic flow. The basic flow exhibits a highly stable nature for $N = -1$, irrespective of the value of media permeability. The chemical reaction parameter in terms of Damkohler number (k) tends to stabilize the flow in high permeability porous medium whereas it has opposite effect in the case of relatively low permeability porous medium.

DATA AVAILABILITY

The data that support the findings of this study are available from the corresponding author upon reasonable request.

Declaration of Competing Interest

Both the authors are neither affiliated nor involved in an organization or entity with a financial or non-financial interest in the subject matter or materials discussed in this manuscript (such as honoraria; educational grants; participation in speakers' bureaus; membership, employment, consultancies, stock ownership, or other equity interest; and expert testimony or patent-licensing arrangements), or non-financial interest (such as personal or professional relationships, affiliations, knowledge or beliefs) that might be affected by publication of the results contained in this manuscript. The authors ensure that no contractual relations or proprietary considerations exist that would affect the publication of information in a submitted manuscript.

Also, this article has not been submitted in any other archive journal as well as conference.

Author Contribution Declaration

Both the authors have equally contributed to the article and also read and approved the final manuscript.

Funding

One of the authors is grateful to DST SERB India for providing financial support [file number: CRG/2022/000419] during the preparation of this manuscript.

ORCID

Aakash Kumar https://orcid.org/0000-0002-9356-5750
Abhishek K. Sharma https://orcid.org/0000-0002-9774-5820

REFERENCES

[1] J. A. Chamkha, "Double diffusive convection in a porous enclosure with coopperating temperature and concentration gradients and heat generation or absorption effects," Numerical Heat Transfer, vol. 41, pp. 65–87, 2002.

[2] N. P. Kaloni and J. Guo, "Steady nonlinear double-diffusive convection in a porous medium based upon the brinkman]forchheimer model," Journal of Mathematical Analysis and applications, vol. 204, pp. 138–155, 1996.

[3] V. Steinberg and H. Brand, "Convective instabilities of binary mixtures with fast chemical reaction in a porous medium," *Journal of Chemical Physics*, vol. 78, no. 5, pp. 2655–2660, 1983.

[4] M. K. Khandelwal, A. K. Sharma, and P. Bera, "Instability of mixed convection in a differentially heated channel filled with porous medium: A finite amplitude analysis," P*hy. of Fluids*, vol. 32, pp. 024109–1–16, 2021.

[5] P. Bera, S. Pippal, and A. K. Sharma, "A thermal non-equilibrium approach on double-diffusive natural convection in a square porous-medium cavity," Int. J. of Heat and Mass Transfer, vol. 78, pp. 1080–1094, 2014.

[6] W. M. Yan, L. Y. Tsay, and T. F. Lin, "Simultaneous heat and mass transfer in laminar mixed convection flows between vertical parallel plates with asymmetric heating," Int. J. Heat Fluid flow, vol. 10, pp. 262–269, 1989.

[7] W. M. Yan and T. F. Lin, "Effects of wetted wall on laminar mixed convection in a vertical channel," Int. J. Heat Fluid flow, vol. 3, pp. 94–96, 1989.

[8] W. M. Yan and H. C. Tsay, "Binary diffusion and heat transfer in laminar mixed convection channel flow with uniform wall heat flux: Extremely thin film thickness," Int. J. Heat Mass Transfer, vol. 26, pp. 23–31, 1991.

[9] W. M. Yan, L. Y. Tsay, and T. F. Lin, "Evaporative cooling of liquid film through interfacial heat and mass transfer in a vertical channel-i. experimental study," Int. J. Heat Mass Transfer, vol. 34, pp. 1105–1111, 1991.

[10] W. M. Yan, "Mixed convection heat and mass transfer in a vertical channel with film evaporation," Can. J. Chem. Eng., vol. 71, pp. 54–62, 1993.

[11] W. M. Yan, "Effects of film vaporization on turbulent mixed convection heat and mass transfer in a vertical channel," Int. J. Heat Mass Transfer, vol. 38, pp. 713–722, 1995.

[12] L. Y. Tsay, "Effects of binary mixture condensation on turbulent mixed convection heat and mass transfer in a vertical channel," Numer. Heat Transfer, Part A, vol. 29, pp. 599–612, 1996.

[13] M. Feddaoui, A. Mir, and E. Belahmidi, "Numerical simulation of mixed convection heat and mass transfer with liquid film cooling along an insulated vertical channel," Heat Mass Transfer, vol. 39, pp. 445–453, 2003.

[14] K. G. Boulama, N. Galanis, and J. Orfi, "Heat and mass transfer between gas and liquid streams in direct contact," Numer. Heat Transfer, Part A, vol. 47, pp. 3669–3681, 2004.

[15] Z. A. Hammou, A. Benhamou, N. Galanis, and J. Orfi, "Laminar mixed convection of humid air in a vertical channel with evaporation or condensation at the wall," Int. J. Therm. Sci., vol. 43, pp. 531–539, 2004.

[16] N. Laaroussia, G. Lauriat, and G. Desrayaud, "Effects of variable density for film evaporation on laminar mixed convection in a vertical channel," Int. J. Heat Mass Transfer, vol. 52, pp. 151–164, 2009.

[17] O. Oulaid, B. Benhamou, and N. Galanis, "Flow reversal in combined laminar mixed convection heat and mass transfer with phase change in a vertical channel," Int. J. Heat Fluid Flow, vol. 31, pp. 711–721, 2010.

[18] A. Cherif, M. A. Kassim, B. Benhamou, S. Harmande, J. Corriou, and S. Jabrallah, "Experimental and numerical study of mixed convection heat and mass transfer in a vertical channel with film evaporation," Int. J. Thermal Science, vol. 50, pp. 942–953, 2011.

[19] El-Din and M. M. S., "Fully developed forced convection in a vertical channel with combined buoyancy forces," Int. Commun. Heat Mass Transfer, vol. 19, pp. 239–248, 1992.

[20] J. A. Chamkha, "Mhd flow of a uniformly stretched vertical permeable surface in the presence of heat generation/absorption and a chemical reaction," Int. Communication in Heat and Mass Transfer, vol. 30(3), pp. 413–422, 2003.

[21] H. C. Chen, "Combined heat and mass transfer in mhd free convection from a vertical plate ohmic heating and viscous dissipation.," Int. Journal of Engineering and Sciences, vol. 42(7), pp. 699–713, 2003.

[22] K. Boulama and N. Galanis, "Analytical solution for fully developed mixed convection between parallel vertical plates with heat and mass transfer," ASME J. Heat Transfer, vol. 126, pp. 381–388, 2004.

[23] K. G. Boulama, N. Galanis, and J. Orfi, "Entropy generation in a binary gas mixture in the presence of thermal and solutal mixed convection," Int. J. Therm. Sci., vol. 45, pp. 51–59, 2006.

[24] K. G. Boulama, N. Galanis, and J. Orfi, "Thermosolutal mixed convection and flow-reversal in an inclined parallel-plate channel," Heat Mass Transfer, vol. 48, pp. 1601–1613, 2012.

[25] D. Pritchard and C. N. Richardson, "The effect of temperature-dependent solubility on the onset of thermosolutal convection in a horizontal porous layer," J. *Fluid Mech.*, vol. 571, pp. 59–95, 2007.

[26] T. Grosan, R. Pop, and I. Pop, "Thermophoretic deposition of particles in fully developed mixed convection flow in a parallel-plate vertical channel," Heat Mass Transfer, vol. 45, pp. 503–509, 2009.

[27] T. K. Aldoss and M. A. Al-Nimir, "Effect of the local acceleration term on the mhd transient free convection flow over a vertical plate.," Int. J. for Numerical Methods for Heat Fluid Flow, vol. 15(3), pp. 296–305, 2005.

[28] J. Zueco and S. Ahmed, "Combined heat and mass transfer by mixed convection mhd flow along a porous plate with chemical reaction in presence of heat source," Appl. Math. Mech.-Engl., vol. 31(10), pp. 1217–1230, 2010.

[29] M. S. Malashetty and B. S. Biradar, "The onset of double diffusive reaction-convection in an anisotropic porous layer," P*hy. of Fluids*, vol. 23, pp. 064102–1–12, 2011.

[30] A. R. Mohammed, O. A. Abdel-Naseer, and M. S. Abo-Dahab, "Unsteady mhd double-diffusive convection boundary-layer flow past a radiate hot vertical surface in porous media in the presence of chemical reaction and heat sink," Meccanica, vol. 48, pp. 931–942, 2013.

[31] M. K. Khandelwal, N. Singh, A. K. Sharma, and P. Yu, "Instabilities during convection diffusion of binary mixtures in a non-isothermal flow: A linear stability analysis," P*hy. of Fluids*, vol. 33, pp. 084107–1–17, 2021.

[32] S. Whitaker, "The forchheimer equation: A theoretical development," T*ransp. Porous Media*, vol. 25, pp. 27–61, 1996.

[33] M. Kaviany, *Principles of Heat Transfer in Porous Media*. New York: Springer, 1991.

[34] G. P. Drazin and H. W. Reid, *Hydrodynamic stability*. Cambridge University Press, 2004.

[35] J. E. Hart, "Stability of the flow in a differentially heated inclined box," *Journal of Fluid Mechanics*, vol. 47, no. 3, p. 547–576, 1971.